doi:10.1016/j.jmb.2004.04.020 J. Mol. Biol. (2004) 339, 681–693

JMB

Available online at www.sciencedirect.com

SCIENCE DIRECT®

ELSEVIER

Structural and Functional Characterization on the Interaction of Yeast TFIID Subunit TAF1 with TATA-binding Protein

Tapas K. Mal[1], Yutaka Masutomi[1], Le Zheng[1], Yasuto Nakata[2] Hiroshi Ohta[2], Yoshihiro Nakatani[3], Tetsuro Kokubo[4] and Mitsuhiko Ikura[1]*

[1]*Division of Molecular and Structural Biology, Ontario Cancer Institute and Department of Medical Biophysics, University of Toronto, Toronto, Ont. M5G 2M9, Canada*

[2]*Division of Gene Function in Animals, Nara Institute of Science and Technology, 8916-5 Takayama, Ikoma 630-0101 Japan*

[3]*Dana-Farber Cancer Institute and Harvard Medical School Boston, MA 02115, USA*

[4]*Division of Molecular and Cellular Biology, Graduate School of Integrated Science Yokohama City University 1-7-29 Suehiro-cho Tsurumi-ku, Yokohama 230-0045, Japan*

**Corresponding author*

General transcription factor TFIID, consisting of TATA-binding protein (TBP) and TBP-associated factors (TAFs), plays a central role in both positive and negative regulation of transcription. The TAF N-terminal domain (TAND) of TAF1 has been shown to interact with TBP and to modulate the interaction of TBP with the TATA box, which is required for transcriptional initiation and activation of TATA-promoter operated genes. We have previously demonstrated that the *Drosophila* TAND region of TAF1 (residues 11–77) undergoes an induced folding from a largely unstructured state to a globular structure that occupies the DNA-binding surface of TBP thereby inhibiting the DNA-binding activity of TBP. In *Saccharomyces cerevisiae*, the TAND region of TAF1 displays marked differences in the primary structure relative to *Drosophila* TAF1 (11% identity) yet possesses transcriptional activity both *in vivo* and *in vitro*. Here we present structural and functional studies of yeast TAND1 and TAND2 regions (residues 10–37, and 46–71, respectively). Our NMR data show that, in yeast, TAND1 contains two α-helices (residues 16–23, 30–36) and TAND2 forms a mini β-sheet structure (residues 53–56, 61–64). These TAND1 and TAND2 structured regions interact with the concave and convex sides of the saddle-like structure of TBP, respectively. Present NMR, mutagenesis and genetic data together elucidate that the minimal region (TAND1 core) required for GAL4-dependent transcriptional activation corresponds to the first helix region of TAND1, while the functional core region of TAND2, involved in direct interaction with TBP convex α-helix 2, overlaps with the mini β-sheet region.

Keywords: general transcription factor; transcriptional regulation; TAF; TBP; TFIID

Introduction

TFIID is a multi-subunit general transcription factor required for transcriptional initiation and regulation of class II genes.[1–4] It consists of TATA box-binding protein (TBP) and TBP-associated factors (TAFs). TBP binds specifically to the TATA element, whereas TAFs bind directly and indirectly to other core promoter elements such as the initiator and downstream promoter element.[5–7] In

Supplementary data associated with this article can be found at doi: 10.1016/j.jmb.2004.04.020

Present addresses: Yutaka Masutomi, Nippon Shinyaku, 14-1 Sakura 3-Cyome, Tsukuba, 305-0003, Japan; Yasuto Nakata, GlaxoSmithKline, 6-15 Sendagaya 4-chome, Shibuya-ku, Tokyo 151-8566, Japan; Hiroshi Ohta, JCR Pharmaceuticals, 3-19, Kasuga-cho, Ashiya, Hyogo, 659-0021, Japan.

Abbreviations used: TBP, TATA-binding protein; TAF, TBP-associated factor; UAS, upstream activating sequence; PCR, polymerase chain reaction; TAND, TAF N-terminal domain; NMR, nuclear magnetic resonance; HSQC, heteronuclear single quantum coherence; CSI, chemical shift index; DBD, DNA-binding domain; AD, activation domain; RPS5, small ribosomal subunit protein 5.

E-mail address of the corresponding author: mikura@uhnres.utoronto.ca

TATA containing promoters, TAFs play crucial roles in facilitating transcription in response to various types of activators.[2,3] In many promoters including the oncogene cyclin D1, the TATA element is absent and TAFs may be more actively involved in the recruitment of TFIID to promoter sequences.[8]

In *Saccharomyces cerevisiae*, TAFs consist of 14 protein subunits. The second largest subunit, yTAF1, previously known as $yTAF_{II}145$ is thought to serve as a platform for the assembly of the entire TFIID complex.[7,9] Among the presumptive multiple TBP-binding sites of TAF1, the N-terminal site, designated as TAF N-terminal domain (TAND), has been best characterized.[10–14] Initially, yeast TAND (yTAND) was shown to consist of two subdomains, yTAND1 (residues 10–37) and yTAND2 (residues 46–71), which bind to the concave and convex surfaces of TBP, respectively (Figure 1).[15] More recently, it has been shown that an additional segment, named yTAND3 (residues 82–139), also binds TBP and stimulates transcriptional activation when fused with GAL4 DNA-binding domain[14] in a manner similar to yTAND1 (Figure 1). Importantly, yTAND1 can inhibit TBP binding to the TATA element, thereby suppressing transcriptional activation of certain genes.[10,13,16] In *Drosophila* TAF1 (dTAF1, formally known as $dTAF_{II}230$), the N-terminal 77 residues, which were assigned to dTAND1, bind to the concave surface of TBP, forming a structure[17] that resembles the TBP-bound TATA box structure with respect to the molecular surface characteristics (Figure 1). dTAND2 (residues 82–156) also participates in TBP binding and augments the inhibitory effect of dTAND1 (Figure 1). dTAND2 interacts on the convex surface of the TBP saddle structure and is shown to compete for the same TBP-binding surface as TFIIA.[13,18,19]

Our early work on *Saccharomyces cerevisiae* showed that the yTAF1 gene lacking yTAND1 or yTAND2 resulted in a temperature sensitive growth phenotype, underscoring the physiological importance of these domains in yTAF1.[15] Genome-wide analysis in yeast[16] revealed a role of yTAND as a primary inhibitor of transcription of some specific genes. On the contrary, TAND also participates in transcriptional activation. In yeast cells, the deletion of TAND1 (ΔTAND1) impairs the activating function of RPS5-UAS and 2x synthetic GAL4-binding sites on the RPS5 core promoter.[20] More intriguingly, ΔTAND1 dramatically increases transcription when some Mediator components,[21] viewed as modulator connecting diverse gene-specific regulatory proteins to the basal Pol II transcriptional apparatus, are artificially recruited.[20] Since pre-recruitment of Mediator by an activator, in the absence of TFIID, decreases PIC assembly and transcription[22] *in vitro*, we suppose that Mediator recruitment by itself is not sufficient to relieve an inhibitory effect of TAND1 and that inhibitory effect of TAND1 should be relieved by the concurrent actions of an activator and Mediator.

Despite the similar function of the N-terminal domain of TAF1 in both yeast and *Drosophila*, the primary sequence of this yTAF1 region significantly differs from that of dTAF1 (sequence identity 17%). In order to understand the structure–function relationship of these evolutionary diverse TAND domains in TAF1, we have undertaken structural studies of TBP interactions with

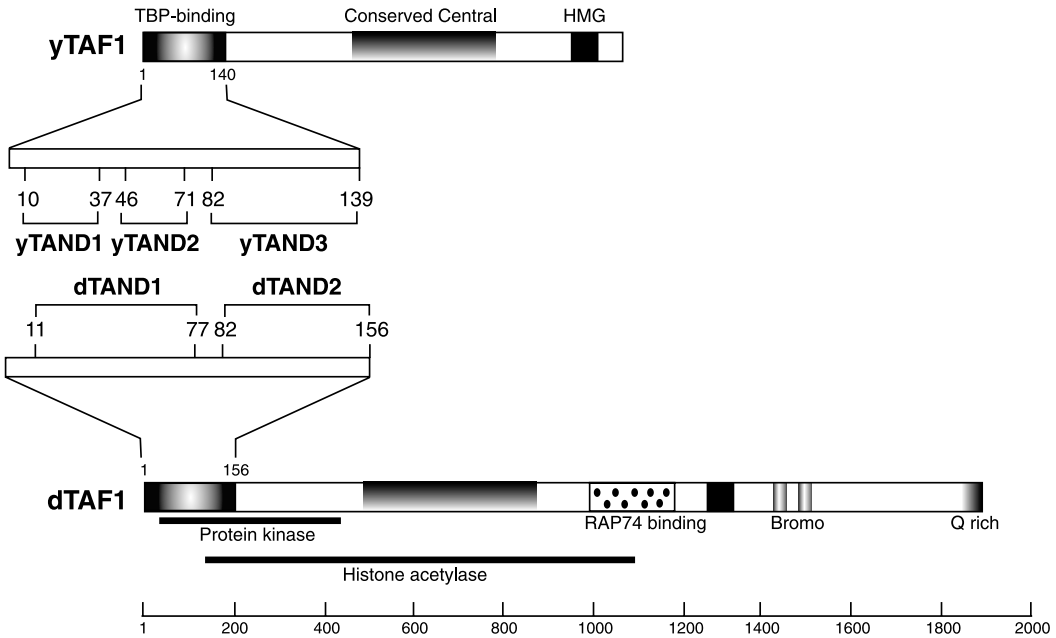

Figure 1. Schematic domain architecture of yTAF1 and dTAF1. TAF1 N-terminal domain (TAND) that binds to TBP can be subdivided into three subdomains (yTAND1, yTAND2 and yTAND3) in the case of yTAF1 and two subdomains (dTAND1 and dTAND2) in the case of dTAF1.

yTAF1 by high resolution nuclear magnetic resonance (NMR) spectroscopy. The present NMR study maps perturbed residues on TBP upon binding of $yTAF1_{10-73}$ as compared with our reported data on TBP–$dTAF1_{11-77}$ complex.[17] Mutagenesis and yeast two-hybrid experiments show that yTAND1 interacts with the TATA box-binding surface of TBP and yTAND2 binds to the TBP convex surface. The minimal region (residues 17–31) of yTAND1 required for transcriptional activation and cell growth has been characterized by deletion mutagenesis studies. These functional data are in excellent agreement with the structural characterization of the TBP–yTAF1 interaction by NMR.

Results

TBP retains a saddle-like structure upon binding of $yTAF1_{10-73}$

Previous mutagenesis and deletion studies have shown that yTAF1 requires both yTAND1 and yTAND2 subdomains for formation of a stable complex with TBP while in the case of dTAF1 subdomain I (dTAND1) is sufficient for interaction.[13,17] yTAND1 is much shorter in polypeptide length compared to dTAND1 and again the sequence homology between them is remarkably poor (11% sequence identity). In order to characterize the interactions of $yTAF1_{10-73}$ on TBP, we have studied TBP–$yTAF1_{10-73}$ complex using mutagenesis and high resolution NMR.

To examine the binding effects of $yTAF1_{10-73}$ on TBP, we first recorded a $^{1}H-^{15}N$ HSQC spectrum of TBP in complex with $yTAF1_{10-73}$. The $^{1}H-^{15}N$ HSQC experiment of uniformly ^{15}N-labeled TBP in complex with unlabeled $yTAF1_{10-73}$ produces a well resolved spectrum (Figure 2A). Comparison of HSQC spectra of free TBP and TBP in complex with $yTAF1_{10-73}$ is not possible because free TBP at a ~ mM concentration is unstable and precipitates readily under the employed NMR conditions.[17] Backbone resonance assignments for C^{α}, C^{β}, ^{15}N and ^{1}H of TBP in complex with unlabeled $yTAF1_{10-73}$ are accomplished using uniformly $^{2}H,^{13}C,^{15}N$-labeled TBP. Secondary structural elements are analyzed using a modified weighted chemical shift indices (CSI) accounting for the possible contribution of C^{α} and C^{β} chemical shifts of a residue at i position with two flanking residues ($i-1$ and $i+1$ positions) in the sequence (Figure 3). A preponderance of positive and negative values for four or more consecutive residues indicates that the TBP structure contains both α helices and β strands. A comparison of TBP–$yTAF1_{10-73}$ and TBP–$dATF1_{11-77}$ complexes[17] indicates no major changes in the secondary structural elements of TBP. However, lengths of α-helix 1, β2′ and β4′ are increased while β5 and β6′ are decreased by one or two residues in the TBP–$yTAF1_{10-73}$ complex when compared with TBP–$dTAF1_{11-77}$ complex (Figure 3). Chemical shifts of ^{15}N and ^{1}H resonances for most residues do not change from our previous data on the TBP–$dTAF1_{11-77}$ complex, with the exception of a few residues discussed below in detail. General observation indicates that TBP retains its saddle-like structure as observed in TBP–$dTAF1_{11-77}$[17] and TBP–DNA[23,24] binary complexes.

To analyze the chemical shift changes quantitatively, we have used the normalized weighted

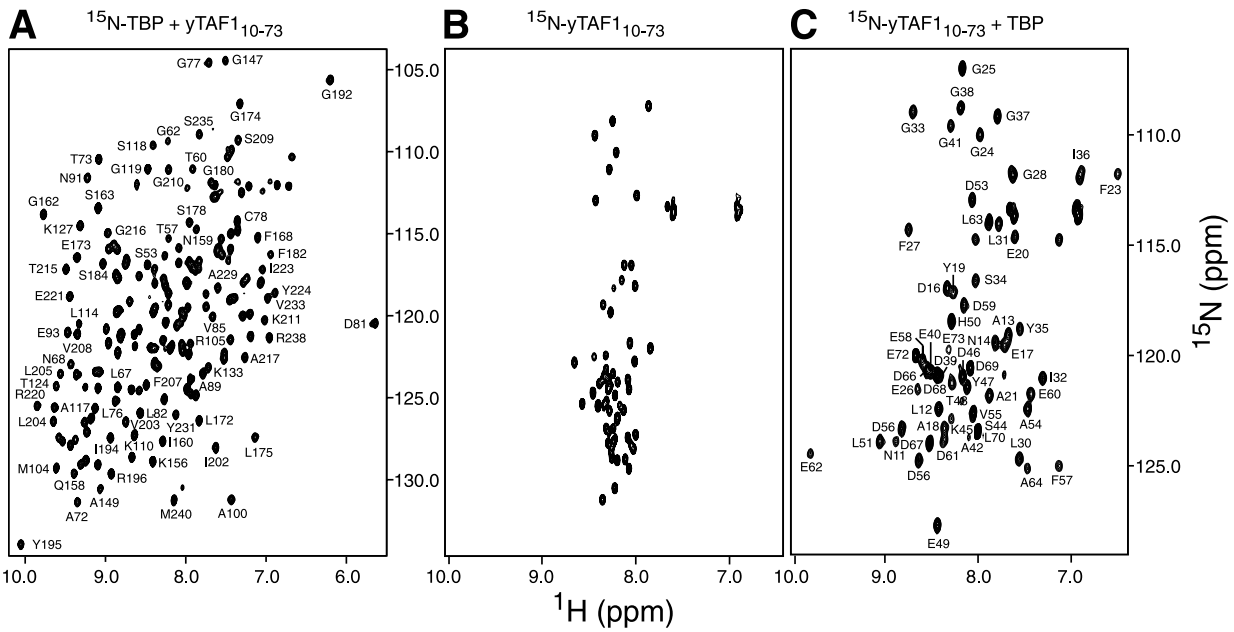

Figure 2. $^{1}H-^{15}N$ HSQC spectra of uniformly labeled (A) TBP in complex with unlabeled $yTAF1_{10-73}$, (B) $yTAF1_{10-73}$ and (C) $yTAF1_{10-73}$ in complex with unlabeled TBP. In A and C several peaks are labeled using the one-letter amino acid representation with a residue number. Poor dispersion of chemical shifts indicates $yTAF1_{10-73}$ is unfolded (B) and undergoes induced folding upon binding to TBP (C).

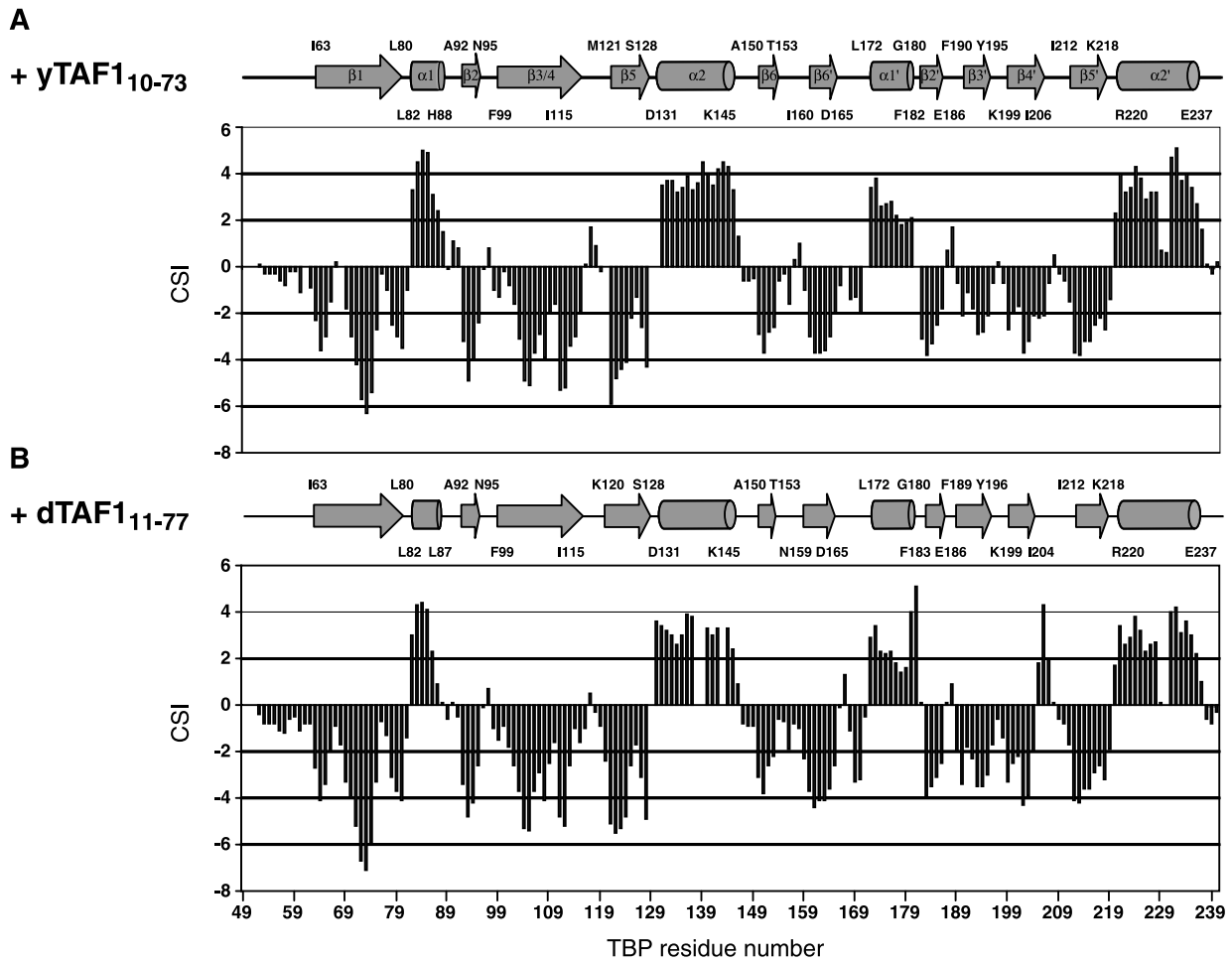

Figure 3. $^{13}C^{\alpha}-^{13}C^{\beta}$ Chemical shift indexes (CSI) plot of TBP in complex with (A) $yTAF1_{10-73}$ and (B) $dTAF1_{11-77}$ plotted against residue number. Four or more consecutive positive CSI values indicate a helix, while negative values indicate a β strand. Putative secondary structural elements labeled with a residue number based on CSI values are shown on top of each diagram. No major differences are observed in the secondary structural elements of TBP in complex with either $yTAF1_{10-73}$ or $dTAF1_{11-77}$ indicating that the overall structure of TBP remains the same with minor local conformal change.

average chemical shift differences ($\Delta_{ave}/\Delta_{max}$) for ^{1}H, ^{15}N, C^{α} and C^{β} chemical shifts of TBP in complex with $yTAF1_{10-73}$ and $dTAF1_{11-77}$ (dTAND1)[25] (see Materials and Methods). $\Delta_{ave}/\Delta_{max}$ provides a means of mapping intermolecular-binding surfaces and defining conformational changes occurring upon binding.[25] The TBP–$dTAF1_{11-77}$ complex[17] provides an excellent platform for comparison of interaction studies of TBP with $yTAF1_{10-73}$ in solution, as NMR study is not possible for free TBP.[19] There are several residues in the TBP–$yTAF1_{10-73}$ complex for which a significant chemical shift change has been observed. The most significant changes are observed for a number of residues including Gln68, Asn69, Leu87, His88, Asn91, Ala100, Leu114, Ser118, Gly125, Lys138, Arg141, Gln144, Gln158, Leu205 and Phe207. In order to get better insight into the location of these perturbed residues, we have mapped them on the TBP structure.[17] Chemical shift perturbations are evident on both convex and concave surfaces of the TBP saddle structure (Figure 4A and B). Interestingly, these residues are largely localized on one half of the 2-fold symmetry TBP structure. Each half contains a pair of short and long α-helices (termed α1 and α2 in the right half, and α1′ and α2′ in the left half in Figure 4B) and only α1 and α2 are affected. Specifically, changes were observed in His88 and Leu87 in α1 while Arg137, Lys138, Arg141, Ile142, Ile143, Gln144, Lys145 and Ile146 in α2. Residues Gln68, Asn69, Val71, Thr73, Ala92, Glu93, Thr111, Leu114, Ile115, Met121, Val122, Gly125, Thr153, Gln158 and Asn159 are part of the β-strands, while Ala89, Arg90, Asn91, Lys97, Phe99, Ala100, Phe116 and Ser118 are from loop regions. Only the concave region of the C-terminal half of TBP structure (left half in Figure 4B) including Leu189, Phe190, Phe207 and Leu205 is perturbed. These results strongly suggest that $yTAF1_{10-73}$ interacts, at least in part, with both the concave and convex regions of TBP and only the N-terminal part of the TBP convex surface is needed for the interaction.

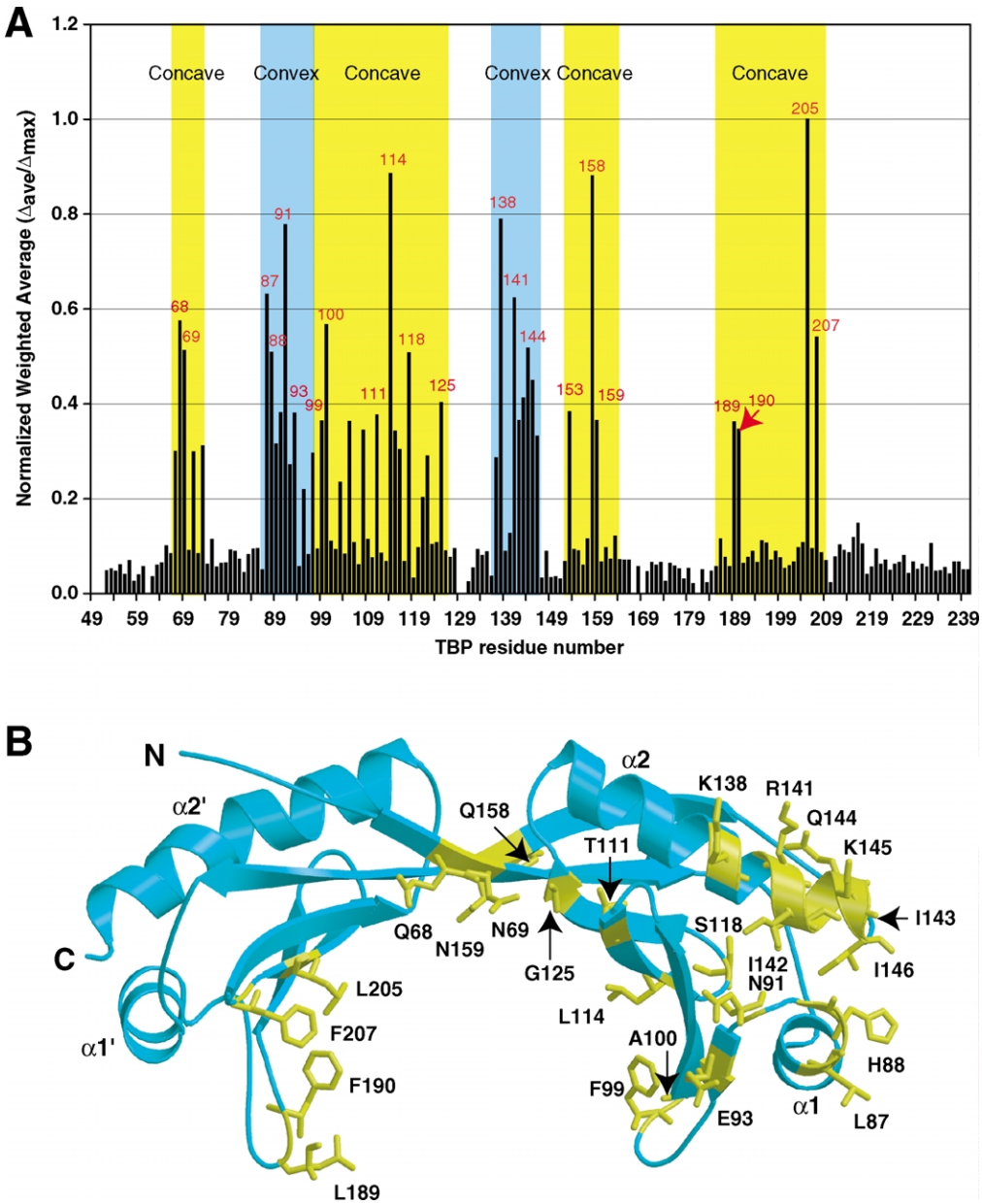

Figure 4. A, Calculated normalized weighted chemical shift differences ($\Delta_{ave}/\Delta_{max}$) of TBP in complex with yTAF1$_{10-73}$ using chemical shift information of the TBP–dTAF1$_{11-77}$ complex[17] are plotted against TBP residue number. Residues with larger chemical shift differences are labeled where possible with a residue number and the parts of concave and convex surface of TBP where residues are affected are represented by yellow and blue shading, respectively. B, Ribbon diagram of TBP taken from the structure of the complex between TBP and dTAF1$_{11-77}$.[17] The most affected residues of TBP upon binding to yTAF1$_{10-73}$ are highlighted with side-chains. The Figure is generated using MOLSCRIPT.[55]

yTAND2 interacts with α-helix 2 on the TBP convex surface

Either yTAND1 or yTAND2 alone does not form a stable complex with TBP, therefore, it is not possible to distinguish which yTAND occupies the TATA box-binding surface of TBP.[15] Our previous mutagenesis and deletion studies have indicated that yTAND1 and yTAND2 recognize the concave and convex surfaces of TBP, respectively.[13,15] This observation is supported by TBP-binding studies involving yTAND fusion subdomain peptides, yTAND1–yTAND1 (y1y1) and yTAND2–yTAND2 (y2y2).[15] Both y1y1 and y2y2 interact with TBP at detectable levels, whereas each individual peptide (yTAND1 or yTAND2) does not, probably because the amounts of TBP recovered on the beads may be doubled. y1y1 binds equally well to both wild-type TBP and mutated TBP (K133E/K138E/K145E), while y2y2 does not bind to mutated TBP nor does yTAND1–yTAND2. Furthermore, y2y2–TBP complex is salt sensitive while y1y1–TBP is

not. These results strongly suggest that yTAND1 recognizes the concave surface of TBP through salt-resistant hydrophobic contacts while yTAND2 is involved in salt-sensitive electrostatic interactions on the convex surface of TBP, including α-helix 2 where mutations are located.[15]

To further confirm that yTAND2 interacts with α-helix 2 of TBP, we have conducted a genetic screen to isolate yTAND mutations that increase interaction with the TBP mutant K138T/Y139A (Supplementary Figure SA and B). We reason that if such mutations are confined to yTAND2 and not found in any other region, yTAND2 must solely be responsible for interaction with the convex surface of TBP. For this purpose, we have exploited the yeast two-hybrid system since the GAL4 DNA-binding domain (DBD) fused to the TBP mutant K138T/Y139A conferred very low background signals unlike wild-type TBP (data not shown). Approximately 60,000 colonies have been transformed with the two plasmids (i.e. one to express GAL4DBD-TBP (K138T/Y139A) and the other to express the GAL4 activation domain (AD)-fused and randomly mutated yTAND), and are screened for growth on 10 mM of 3-amino-triazole (3-AT) containing plates (Figure SB). Plasmids containing suspected yTAND mutations were recovered and reintroduced into the same host strain to confirm the phenotype. Seven yTAND mutants that consistently grow on 3-AT plates (5, 10, 15 mM) were finally isolated. DNA sequencing reveals that they have all contained frame shift mutations that can be classified into three distinct types: 1, 2 and 3 (including four, two and one independent clones, respectively) as shown in Figure 5A. Interestingly, all mutations mapped are within the highly conserved yTAND2 region that has been shown to directly interact with the surface of α-helix 2 of TBP.[15] Since residues in the C-terminal region, beginning from Ala64, are all changed in these mutants, therefore, we consider that one-third of C-terminal yTAND2 may directly recognize or be in close proximity to K138/Y139 residues on α-helix 2. Importantly, these frame shift mutations do not restore the interaction with another TBP mutant (K133E/K138E/K145E) under the same conditions (data not shown) suggesting that the restored interaction is specific for T138/A139 residues. Another intriguing issue is that we cannot isolate any mutations that affect the N-terminal portion of yTAND2 core region. This may be because the amino-terminal region is involved in recognizing other residues on α-helix 2 that are unchanged in the TBP mutant K138T/Y139A. Taken together, we conclude that yTAND2, not yTAND1 recognizes α-helix 2 of TBP.

Identification of a functionally minimal region in yTAND1

To dissect the minimal binding region of yTAND1 (residues 10–37), we have employed transcriptional activation assays using a GAL4 fusion system. We have shown[26] that yTAND1 (residue 10–37) activates transcription of the *GAL1* promoter when it is fused to the GAL4 DBD, indicating that it can function as an activation domain (AD). To identify the minimal region of yTAND1 that can function as an AD, we have constructed a series of truncated mutants as described in Figure 5B (left panel). Deletion of residues 32–37 from the C-terminal portion significantly decreases AD activity (compare constructs 2 and 3) and further deletion of the region containing residues 26–31 completely abolishes AD activity (construct 6). In constrast, deletion of N-terminal residues 10–14 has little effect on AD activity (compare constructs 1 and 7, and constructs 3 and 9). However, further deletion of residues 15–19 abolishes AD activity (compare constructs 7 and 8, and constructs 9 and 15). Interestingly, deletion of two acidic amino acid residues, i.e. Glu15 and Asp16, increases AD activity of construct 9 by more than two-fold when compared to construct 13. It, therefore, appears that these two acidic residues negatively regulate AD activity. Further deletion from either the N or C terminus of construct 13 greatly impairs AD activity. From these results, we conclude that the region containing residues 17–31 is the minimal region required for activation as it furnishes more than 50% of activity of the wild type yTAND1. This finding is in excellent agreement with our previous results where we have employed alanine scanning mutagenesis.[26]

We have then asked whether this minimal yTAND1 activation region (residues 17–31) (Figure 5B) carries any other TAND1 function. We have tested this region for cell growth in yeast. We have shown that yTAND1 is required for normal cell growth of yeast cell[26] at 37 °C (Figure 5C). Deletion of residues 2–16 or 32–40 alone from yTAND1 does not affect growth at either 25 °C or 37 °C (Figure 5C). Simultaneous deletion of these two regions has affected growth slightly but still supported growth at 37 °C. Therefore, the region between residues 17 and 31 is the functionally minimal yTAND1 region required for transcriptional activation and yeast cell growth.

Induced folding of yTAF1$_{10-73}$ upon binding to TBP

To structurally characterize the yTAND region, we have first recorded a $^{1}H-^{15}N$ HSQC spectrum of uniformly ^{15}N–labeled yTAF1$_{10-73}$. The NMR spectrum of free yTAF1$_{10-73}$ has the characteristic of an unfolded peptide (Figure 2B). The NH and $^{1}H\alpha$ resonances are sharp and poorly dispersed, and their chemical shifts do not deviate significantly from random coil values. Upon binding to TBP, the complex produces a well dispersed $^{1}H-^{15}N$ HSQC spectrum (Figure 2C) with an expected number of backbone NH cross-peaks indicating that yTAF1$_{10-73}$ adopts a single folded conformation. This suggests that yTAF1$_{10-73}$

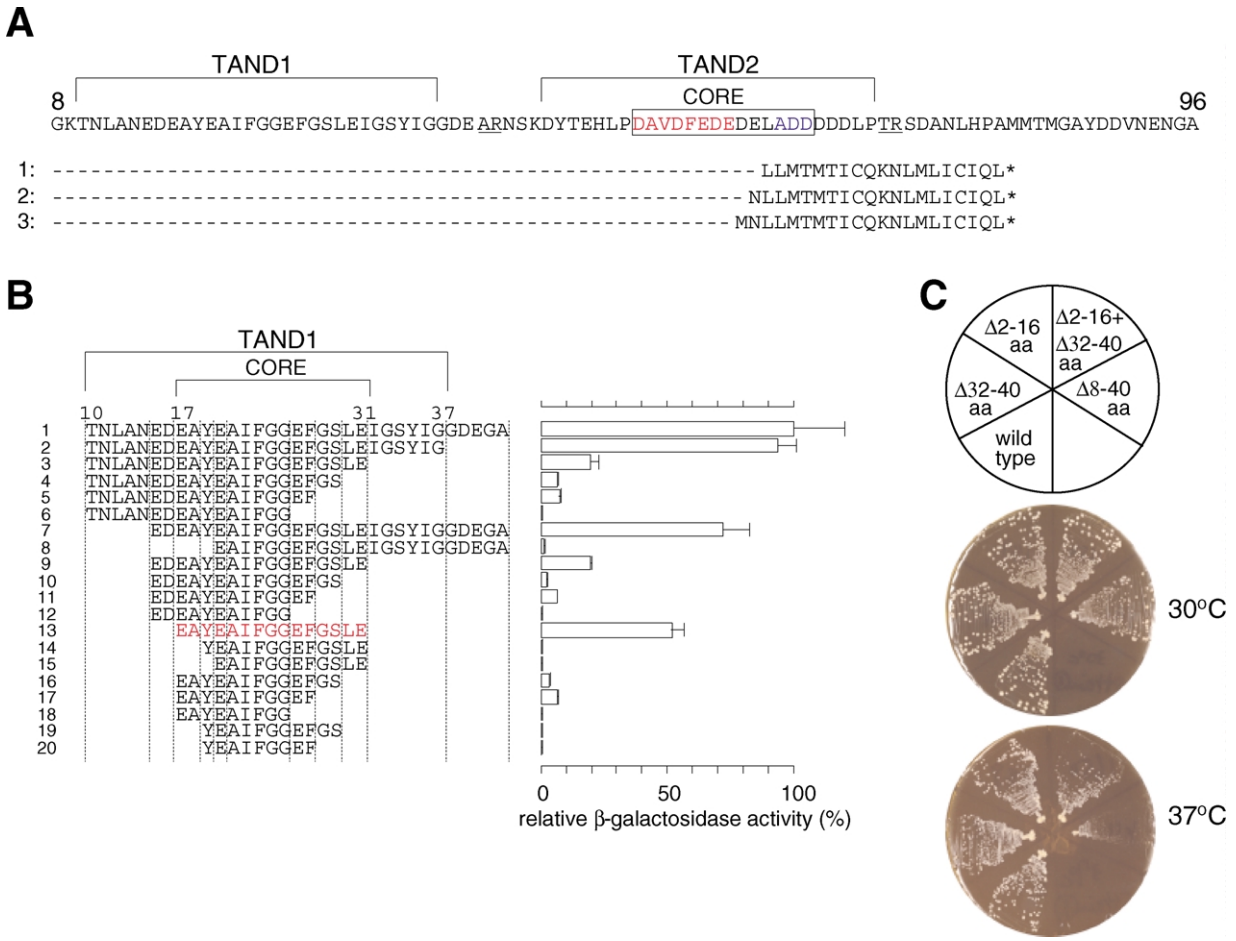

Figure 5. A, Isolation and characterization of yTAND mutations that increase interaction with the TBP mutant K138T/Y139A. Three types of frame shift mutations have been isolated in the genetic screen using the yeast two hybrid system. The number of yTAND mutants for type 1, 2 and 3 are four, two and one, respectively. Notably, each member belonging to the same type 1, 2 and 3 contains the same deletion of one nucleotide, i.e. T189Δ, G184Δ and G181Δ, respectively (numbering here is relative to the A residue of the initiating AUG codon). A broken line and an asterisk denote the same residue as the wild-type and a stop codon, respectively. Changed or unchanged residues within the yTAND2 direct-binding domain required for interaction on TBP convex surface including α-helix 2 are colored in blue and red, respectively. B, Identification of the minimal region of TAF1 peptide required for activator function when it is tethered to DNA by the GAL4 DNA-binding domain (DBD). Amino acid sequences of a series of constructs (constructs 1–20) with a number of deletions in the region between residues 10 and 42 of TAND1 are shown in the left panel. Each construct has been fused to the GAL4 DBD (residues 1–147) and expressed in yeast to measure activator function. The minimal activation domain (AD, residues 17–31) carrying the activator function is shown in red. GAL4-dependent transcriptional activation for each construct in yeast is represented by a horizontal bar (right panel). The expression plasmids described in the left panel have been transformed into the yeast strain SFY526, and the transcriptional activities are determined by measuring *lacZ* reporter activities. β-Galactosidase activity has been calculated as a percentage relative to the full length region (residues 10–42). C, Growth comparison of several *taf1* mutants at 30 and 37 °C. Strains lacking the TAF1 gene but carrying one of several TRP1 marked plasmids encoding TAF1 derivatives as indicated are grown on YPD plates for three days at the indicated temperatures.

undergoes an induced folding from random coil to folded conformation upon binding to TBP.

Chemical shifts for backbone C^{α}, C^{β}, ^{15}N and ^{1}H of $yTAF1_{10-73}$ are assigned using uniformly ^{2}H, ^{13}C, ^{15}N-labeled $yTAF1_{10-73}$ in complex with unlabeled TBP. CSI has been calculated using C^{α} and C^{β} chemical shifts for each residue of $yTAF1_{10-73}$ (Figure 6). CSI values obtained for $yTAF1_{10-73}$ indicate that yTAND1 contains two α helices (α1, residue 16–23; α2, 30–36) and yTAND2 possesses a mini β-sheet structure (residues 53–64; β1, 53–56; β2, 61–64) with a four residue linker between the two strands. In contrast, our previous study of dTAND1 in complex with TBP[17] showed that dTAND1 is comprised of three α helices and a β-hairpin-like structure (Figure 7B).

It is noteworthy that several resonances in the HSQC spectrum of ^{15}N-labeled $yTAF_{10-73}$ in complex with unlabeled TBP are broader than the rest. These residues include Phe23, Glu26, Ala42, Lys45, Thr48, Phe57, Asp61, Glu62, Ala64, Asp67 and Glu73. Many of these residues are located in yTAND2 region. Interestingly, the perturbed amino acid residues, including Lys138, Arg141,

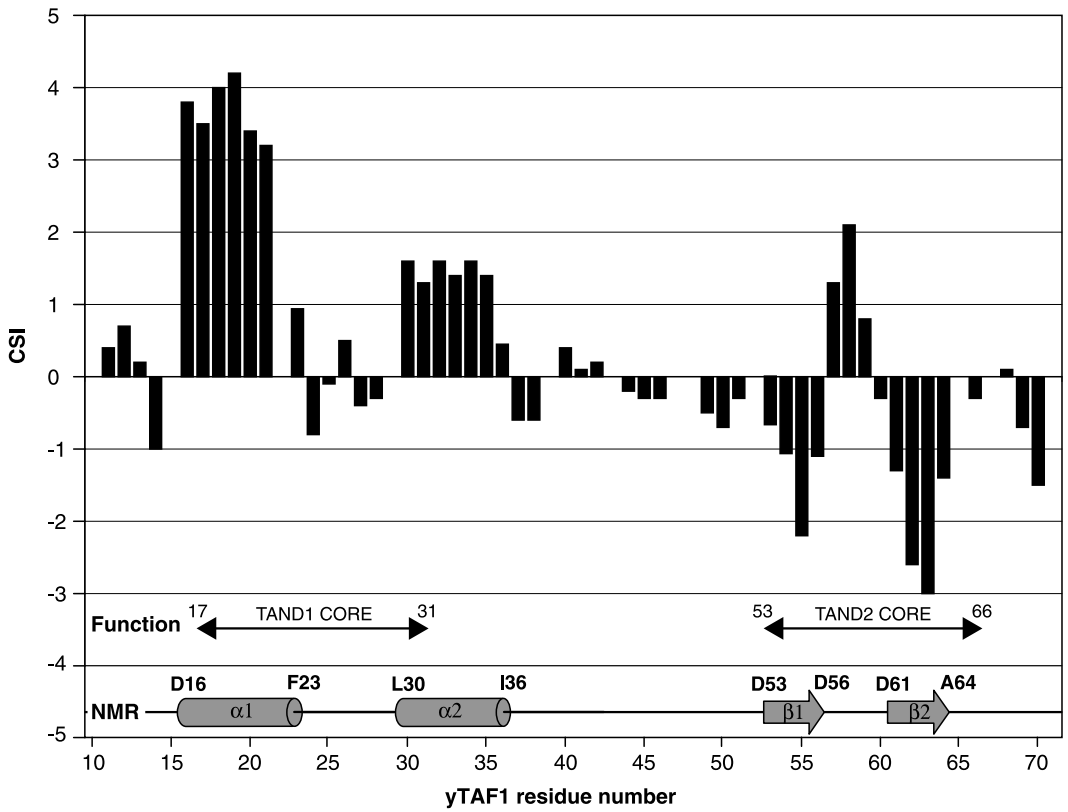

Figure 6. $^{13}C^{\alpha}-^{13}C^{\beta}$ Chemical shift index (CSI) plot of $yTAF1_{10-73}$ in complex with unlabeled TBP plotted against residue number. Putative secondary structural elements based on CSI values are plotted next to the *x*-axis at bottom of the plot. Extent of each structural elements are indicated using the one-letter amino acid code with a residue number. The minimal functional regions of yTAND1 (TAND1 CORE) and yTAND2 (TAND2 CORE) are represented by arrows. TAND1 CORE corresponds to the functional core region required for minimal AD, while TAND2 CORE represents the functional core, essential for direct interaction with TBP convex surface including α-helix 2.

Lys145 on α-helix 2 of TBP, are basic in nature. This is perhaps not surprising that yTAND2 contains a high proportion of acidic amino acid residues (50%) compared to 21% in yTAND1 (Figure 7C). It is therefore, highly plausible that the interaction between yTAND1 and TBP is dominated by hydrophobic contacts while the yTAND2–TBP interaction is influenced by electrostatic contacts given the amphipathic, basic nature of the C-terminal half of TBP α-helix 2. Our previous studies suggest that both acidic and hydrophobic residues in yTAND1 are important for TBP interaction while mutation of acidic residues in yTAND2 severely reduces TBP binding.[13] Furthermore, we have shown that Phe57 is essential for TBP interaction.[15] Hence, yTAND2 also makes hydrophobic contacts with TBP but to a lesser extent than yTAND1. Taken together, these results suggest that it is possible that the two subdomains, yTAND1 and yTAND2 of $yTAF1_{10-73}$, simultaneously bind TBP with different time-scales of chemical exchange between bound and unbound forms, and hence contribute to resonance broadening of residues located in the yTAND2 region. Interactions of a similar nature have been observed in the TBP–$dTAF_{11-156}$ complex.[19]

Discussion

In order to prevent cells from transcribing unnecessary genes or to initiate transcription of necessary genes, cells have developed various mechanisms to regulate gene transcription. This is partly accomplished by the chromatin modifying/remodeling mechanism in which the chromatin structure prevents access of the general transcription machinery to the core promoter.[27–29] Other mechanisms of transcriptional repression include the regulation of TBP interactions with promoter DNA, which appears a pivotal intermediary step in transcriptional activation and deactivation.[30] Once bound to DNA directly or indirectly, TBP is capable of nucleating transcription complex assembly at the TATA containing or even TATA less promoter. Regulatory proteins such as Mot1[31,32] and NC2[33,34] act on the TBP–DNA complex, preventing proper assembly of other general transcription factors. Dimerization of TBP *via* the concave surface, which inhibits TBP binding to the TATA box, is also known to play a role in such TBP-dependent transcriptional repression.[16,35] Indeed, this has been supported by a recent study by Kou *et al.* involving extensive mutation at the dimeric interface of yTBP.[35] Finally, TAF1 is also

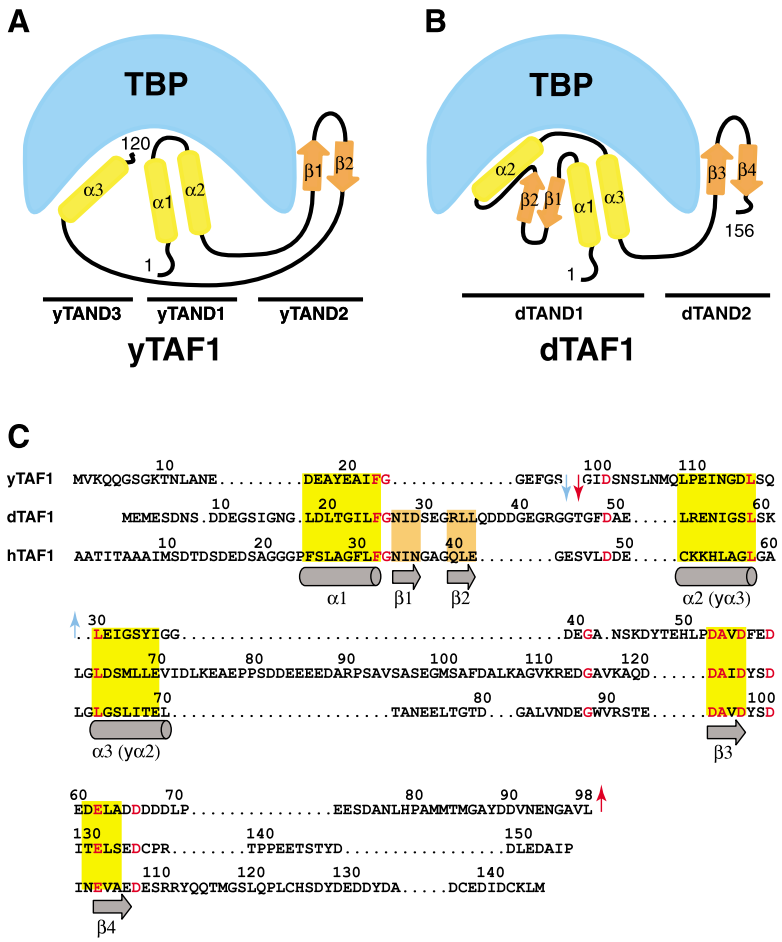

Figure 7. A model of (A) TBP–yTAF1 and (B) TBP–dTAF1 complexes showing a possible relationship between yTAND and dTAND structural elements. TBP is shown in blue while TAF1 secondary structural elements with helices and β strands are shown in yellow and orange, respectively. Schematic domain boundaries (TAND) on the N-terminal yTAF1 and dTAF1 are shown below each diagram. yTAND1 α1 and α2 helices correspond to α1 and α3 helices of dTAND1 and yTAND2 β1 and β2 correspond to dTAND2 β3 and β4. We speculate that yTAND3 may form an α-helix (α3) that mimics α2 helix within dTAND1. This "internal domain shuffling" may have occurred between yeast and *Drosophila*. C, Sequence alignment of the N-terminal region of TAF1 from yeast (yTAF1), *Drosophila* (dTAF1) and human (hTAF1) based on structural and mutational studies.[14] Residues in yellow shades represent putative common secondary structural regions among these proteins assigned according to the structure of $dTAF1_{11-77}$[17] and identical residues are colored in red. yα2 and yα3 represent yeast α2 and α3, respectively, and are equivalent to α3 and α2 of $dTAF1_{11-77}$. The region including α2 of yTAF1 (residues 99–118) is superimposed on residues 47–61 from dTAF1 and residues 46–60 from hTAF1. The break in alignment of the yTAF1 sequence is indicated by blue colored arrows while red colored arrows represent the insertion.

known to prevent TBP from binding to the TATA element by virtue of its N-terminal region, which directly interacts with the concave surface of TBP.[10,17,19,36,37] Although this TBP-binding region of TAF1 is functionally conserved from yeast to *Drosophila* to mammals, the sequence similarity between yeast and *Drosophila* is markedly low (17% identity), leaving one to wonder how they are functionally conserved.

The yTAND1 region, although much shorter in length than its counterpart in dTAND1, has also been suggested to interact with the concave surface of TBP.[13] Unlike dTAND1, the transcriptional repression function of yTAND1 is dependent on an adjacent yTAND2 region, and again the TBP residues involved in yTAND interaction have not been fully identified.[35] Moreover, the recently discovered yTAND3 region in yTAF1 has been shown to overlap with yTAND1-binding site on the TBP concave surface, making it difficult to reconcile current knowledge on the interaction between TBP and yTAND. In our NMR studies,[17,19] we have shown that (i) dTAND1 occupies the DNA binding concave surface of TBP, such that it engages molecular mimicry of the TATA box by many hydrophobic amino acid residues, and (ii) that dTAND2 region interacts with the convex surface of TBP, namely involving K133 and R141 on α-helix 2. In the present study, we have shown that $yTAF1_{10-73}$ perturbs both the concave and convex areas of TBP in a similar manner to that observed in $dTAF1_{1-156}$.[19] In $yTAF1_{10-73}$, two α-helices (residues 16–23 and 30–36) in yTAND1 and an antiparallel mini β-sheet in yTAND2 (residues 53–64) form a core structural unit in respective subdomain. Interestingly, the minimal region (residues 17–31) required for GAL4-dependent AD function (Figure 5B) and yeast cell growth (Figure 5C) coincides with the two α-helices identified from our NMR studies (Figure 6). On the other hand, the mini β-sheet structure found in yTAND2 corresponds to the region responsible for the direct interaction with α-helix 2 of TBP[15] (Figures 5A and 6). Interestingly, this region in TAND2 possesses a high sequence similarity to the corresponding region in *Drosophila* and human[14] (Figure 7C). These results demonstrate how yeast TAND regions function as a suppressor (through the direct interaction with TBP) and an activator (*in vivo* transcription assay) using a similar structural architecture as found in dTAND1.[13,19]

At present the structural basis for transcriptional

stimulation by activation domains is poorly understood except in a few specific cases. Wright and co-workers[38] have elegantly demonstrated that the activation domain of CREB forms a kinked helical structure upon binding to the KIX domain of CBP. Other examples include: (i) the structure of herpes virus VP16 activation domain in the presence of human $TAF_{II}31$[39] and (ii) the structure of p53 activation domain in complex with MDM2.[40] In both cases, the activation domain adopts an α-helical structure upon binding to its binding partner. In parallel with the previous studies,[26] the present biochemical data indicate that yTAND1 can function as an activation domain in the GAL4-dependent transcription assay (Figure 5). The present structural finding that yTAND1 undergoes an induced folding to form a helical structure is fully consistent with the previous structural studies on various activation domains. Furthermore, our findings suggest that the structure observed in yTAND1 bound to TBP concave surface may mimic the structure of an activation domain of transcriptional activators, such as VP16, which has also been shown to interact with the same surface of TBP.[41–44]

The question, however, remains as to how only two helices of yTAND1 occupy the same region as dTAND1 and prevent TBP binding to the TATA promoter. Our GAL4-based transcriptional activation and yeast cell growth assays together with our structural data and previous mutagenesis studies[13,15] provide evidence for the yTAND1 region forming a helical core domain that interacts with the concave surface of TBP. Furthermore, Takahata *et al.*[14] recently reported that yTAND3 interacts with the concave surface of TBP and that a portion of yTAND3 (Leu109–Leu116) displays a high sequence homology to dTAND1 (Leu52–Leu59) (Figure 7C). These results suggest that yTAND3 may mimic the α2 helix of dTAND1 when it binds to TBP (Figure 7). Taken together, it is tempting to speculate that yTAND1 and yTAND3 may constitute a complete structural unit that can occupy the TBP concave surface in a manner similar to the one previously observed in dTAND1[17] (Figure 7). Further biochemical and structural studies are essential to establish a more detailed picture of yeast TAND functions.

Materials and Methods

Protein expression and purification for NMR spectroscopy

The protocols for obtaining the C-terminal core domain (residues 40–240) of *Saccharomyces cerevisiae* TBP (M_r 21.3 kDa) have been described.[17] DNA encoding yTAF1 (residues 10–73) was subcloned into pGEX-2T (Amersham Biosciences) and expressed as a glutathione *S*-transferase (GST) fusion protein. The vector was transformed into BL21(DE3) (Novagen). Cells were grown at 37 °C until an A_{600} of 0.6 and induced with 0.5 mM isopropyl-beta-D-thiogalactopyranoside (IPTG) for five hours. The GST tagged $yTAF1_{10-73}$ protein was purified with glutathione Sepharose (Amersham Biosciences) in 20 mM Tris–HCl (pH 7.5), 5% (v/v) glycerol, 150 mM KCl, 2.5 mM $CaCl_2$, 5 mM DTT. $yTAF1_{10-73}$ was further purified by gel filtration using Superdex 75 (Amersham Biosciences). Isotope-labeled protein samples were obtained by bacterial expression in modified minimal M9 medium supplemented with 1 g/l ^{15}N-ammonium chloride and/or $^{13}C_6$-D-glucose and/or ^2H_2O. Several samples of different labeling types including uniformly ^{15}N-, $^{15}N/^{13}C$- and $^{15}N/^{13}C/^2H$-labeled were prepared for NMR studies.

Preparation of TBP–$yTAF1_{10-73}$ complex

The TBP–$yTAF1_{10-73}$ complex was prepared by slow addition of purified TBP protein solution at low concentration (<0.3 mg/ml) to $yTAF1_{10-73}$ in the presence of 150 mM KCl. Unlabeled protein concentration was always used in excess. The mixed solution was concentrated and applied to a Superdex-75 column to separate unreacted $yTAF1_{10-73}$ and other impurities from the complex in buffer solution of 20 mM Hepes (pH 7.5), 5% glycerol, 150 mM KCl, 5 mM DTT and 1 mM PMSF. The collected sample was then passed through a Mono-S column to further purify the complex from excess and unreacted TBP. The complex did not bind Mono-S and was collected in flow through. The complex was then dialyzed in 20 mM Tris–HCl (pH 7.5), 150 mM KCl, 10 mM $MgCl_2$, 5% glycerol, 0.5 mM AEBSF, 10 mM DTT and 0.05 mM NaN_3 buffer and concentrated using Centricon-10 (Amicon) for NMR studies.

NMR spectroscopy

NMR samples of the TBP–$yTAF1_{10-73}$ complex comprised one isotope labeled and one unlabeled protein with a concentration in the range of 0.8–1.0 mM in 95% H_2O/5% (v/v) ^2H_2O. All NMR experiments were performed at 25 °C on a Varian Inova 600 MHz spectrometer equipped with a triple resonance pulse field gradient probe. $^1H-^{15}N$ heteronuclear single quantum coherence (HSQC) spectra were recorded with 128 and 576 complex points in t_1 and t_2, respectively. Spectral widths were 34 ppm and 14.9 ppm for the ^{15}N (F_1) and ^1H (F_2) dimensions, respectively. Sequential resonance assignments for backbone ^1HN, $^{13}C^\alpha$, $^{13}C^\beta$ and ^{15}N nuclei for both TBP and $yTAF1_{10-73}$ were derived from three-dimensional (3D) HNCA/HN(CO)CA and HN(CA)CB/HN(CO-CA)CB data sets[45] using a ^2H, ^{15}N, ^{13}C labeled sample. NMR data were processed and analyzed using NMRPipe/NMRDraw[46] and XEasy.[47] The secondary structures were analyzed by calculating chemical shift indices (CSI).[48] We used a modified weighted CSI calculation developed in house to account for possible contribution of $^{13}C^\alpha$ and $^{13}C^\beta$ chemical shifts at i position with two flanking residues ($i-1$ and $i+1$ positions) in the sequence.[49] The modified weighted CSI function used as $CSI(C^\alpha,C^\beta) = [(\Delta C^\alpha_{i-1} - \Delta C^\beta_{i-1}) + 2(\Delta C^\alpha_i - \Delta C^\beta_i) + (\Delta C^\alpha_{i+1} - \Delta C^\beta_{i+1})]/4$, where ΔC^α and ΔC^β correspond to the deviation in ppm of C^α and C^β chemical shift values, respectively, from random coil values for the same residue type. Chemical shifts for ^1HN, ^{15}N, C^α and C^β of TBP in complex with $yTAF1_{10-73}$ were compared to those of the TBP–$dTAF1_{11-77}$ complex and analyzed using normalized weighted average chemical shift differences ($\Delta_{ave}/\Delta_{max}$) (calculated from non-zero $\Delta_{ave}/\Delta_{max}$ values).[25] Normalized weighted average chemical shifts[50]

were calculated using $\Delta_{ave}(NHC^{\alpha}C^{\beta}) = [(\Delta H^2 + (\Delta N/5)^2 + (\Delta C^{\alpha}/2)^2 + (\Delta C^{\beta}/2)^2)/4]^{1/2}$ with the exception of glycine and proline residues where Δ_{ave} was calculated as $[(\Delta H^2 + (\Delta N/5)^2 + (\Delta C_{\alpha}/2)^2)/3]^{1/2}$ and $[((\Delta C^{\alpha}/2)^2 + (\Delta C^{\beta}/2)^2)/2]^{1/2}$, respectively.

Construction of GAL4–fusion plasmids

To express various N-terminal portions of TAF1 peptide as GAL4 fusions in yeast cells, pM468, pM889, pM890, pM1099, pM1100, pM891, pM892, pM893, pM1101, pM1102, pM1103, pM1104, pM1105, pM1106, pM1107, pM1108, pM1109, pM1110, pM1111 and pM1112 were constructed by ligating DNA fragments encoding regions lying between 10–42, 10–37, 10–31, 10–29, 10–27, 10–25, 15–42, 20–42, 15–31, 15–29, 15–27, 15–25, 17–31, 19–31, 20–31, 17–29, 17–27, 17–25, 19–29 and 19–27 residues, respectively, into pM471.[51] These fragments were amplified by PCR from pM1169/*TAF1* (*TRP1* marker)[14] using the primer pairs T844 and TK202, T844 and TK398, T844 and TK399, T844 and TK592, T844 and TK593, T844 and TK400, TK401 and TK202, TK402 and TK202, TK401 and TK399, TK401 and TK592, TK401 and TK593, TK401 and TK400, TK594 and TK399, TK595 and TK399, TK402 and TK399, TK594 and TK592, TK594 and TK593, TK594 and TK400, TK595 and TK592, and TK595 and TK593, respectively.

To express TBP mutants that carry a triple K133E/K138E/K145E[13] or a double K138T/Y139A[52] amino acid substitution as GAL4 fusion proteins in yeast cells, DNA fragments amplified by PCR primer pairs, TK21 and TK22 from pET-based TBP expression vectors containing the corresponding mutations, were ligated into pGBT9 (Clontech) to give pM119 and pM120, respectively.

β-Galactosidase assay

Plasmids that express GAL4 fusions, as described above, were transformed into yeast strain SFY526 to measure the transcriptional activation of a chromosomally integrated *lacZ* reporter gene driven by the *GAL1* promoter. They were grown in selective medium and assayed for β-galactosidase activity according to the manufacturer's protocol (Clontech).

PCR mutagenesis and screening for TAND mutations in the yeast two-hybrid system

A sequence of the yTAND region (residues 8–96) of *yTAF1* was amplified from pM34[51] by error-prone PCR[53] using the primer pairs TK143 and TK39 in buffer A (10 mM Tris–HCl (pH 8.3), 50 mM KCl, 7 mM $MgCl_2$, 0.5 mM $MnCl_2$, 300 nM oligonucleotides, 2.6 μg of pM34 DNA per ml, and 100 i.u of *Taq* DNA polymerase per ml) under the following conditions: five minutes at 95 °C; 35 cycles of 30 seconds at 95 °C, 30 seconds at 50 °C, and 90 seconds at 72 °C; and ten minutes at 72 °C. A random mutant library was generated by ligating the resulting error-prone PCR products into the EcoRI/BamHI sites of pGAD424 (Clontech). The plasmid library was transformed into the reporter strain HF7c (Clontech), which already contained pM120, and incubated for one week at 30 °C. Approximately, 60,000 colonies were replica plated onto 3-aminotriazole (3-AT; 10 mM) containing media to screen for yTAND mutants that have increased affinity for the TBP mutant K138T/Y139A. Phenotype reproducibility was tested by picking colonies off the original plates and streaking them on the same plates again. Plasmids containing potential yTAND mutants were rescued and retransformed into HF7c expressing the same TBP mutant (K138T/Y139A). Replica assays on 3-AT plates were repeated, and if the colonies still grew, DNA sequencing was carried out to identify mutational alterations. To test the specificity of the interaction with TBP, plasmids carrying yTAND mutations that increased the interaction with the TBP mutant K138T/Y139A were each co-transformed with pM119, which expressed another TBP mutant (K133E/K138E/K145E) or with an empty vector (pGBT9). Colonies were then replica plated onto 0 mM, 5 mM, 10 mM, 15 mM of 3-AT containing media.

Construction of plasmids encoding TAF1 genes

pM1169 (*TAF1*/pRS314) and pM1002 (*TAF1*Δ*8-40aa*)/pRS314) were constructed by inserting a DNA fragment encoding four repeats of the HA epitope tag at the C terminus of TAF1 peptide encoded by pM11 and pM30,[15] respectively. pM1169 was subjected to site-specific mutagenesis to create pM1648 (*TAF1*Δ(*32-40aa*)/pRS314) and pM1649 (*TAF1*Δ(*2-16aa*)/pRS314) by using oligonucleotides TK1216 and TK1217, respectively. pM1649 was mutagenized to create pM1650 (*TAF1*Δ(*2-16aa*)Δ(*32-40aa*)/pRS314) using the oligonucleotide TK1216.

Yeast strains

Standard techniques were used for yeast growth and transformation.[54] The YTK2741, YTK4688, YTK4691, YTK4694 and YTK2236 strains harboring pM1169, pM1648, pM1649, pM1650 and pM1002, respectively, were generated from Y22.1 (Δ*taf1* strain)[13] by a plasmid shuffle technique.

Acknowledgements

We thank Robert Roeder for providing the original vector used for TBP expression, Joan S. Steffan for advice on error-prone PCR, and Dean Liu and Stefan Bagby for discussions during the initial stage of this study. This work was supported by Canadian Institutes of Health Research (CIHR) grants to M.I. M.I. is a CIHR Senior Investigator.

References

1. Orphanides, G., Lagrange, T. & Reinberg, D. (1996). The general transcription factors of RNA polymerase II. *Genes Dev.* **10**, 2657–2683.
2. Roeder, R. G. (1998). Role of general and gene-specific cofactors in the regulation of eukaryotic transcription. *Cold Spring Harb. Symp. Quant. Biol.* **63**, 201–218.
3. Naar, A. M., Lemon, B. D. & Tjian, R. (2001). Transcriptional coactivator complexes. *Annu. Rev. Biochem.* **70**, 475–501.
4. Lee, T. I. & Young, R. A. (2000). Transcription of eukaryotic protein-coding genes. *Annu. Rev. Genet.* **34**, 77–137.
5. Burke, T. W. & Kadonaga, J. T. (1997). The

downstream core promoter element, DPE, is conserved from *Drosophila* to humans and is recognized by TAFII60 of *Drosophila*. *Genes Dev.* **11**, 3020–3031.
6. Chalkley, G. E. & Verrijzer, C. P. (1999). DNA binding site selection by RNA polymerase II TAFs: a TAF(II)250–TAF(II)150 complex recognizes the initiator. *EMBO J.* **18**, 4835–4845.
7. Sanders, S. L., Garbett, K. A. & Weil, P. A. (2002). Molecular characterization of *Saccharomyces cerevisiae* TFIID. *Mol. Cell. Biol.* **22**, 6000–6013.
8. Hilton, T. L. & Wang, E. H. (2003). Transcription factor IID recruitment and Sp1 activation. Dual function of TAF1 in cyclin D1 transcription. *J. Biol. Chem.* **278**, 12992–13002.
9. Tora, L. (2002). A unified nomenclature for TATA box binding protein (TBP)-associated factors (TAFs) involved in RNA polymerase II transcription. *Genes Dev.* **16**, 673–675.
10. Bai, Y., Perez, G. M., Beechem, J. M. & Weil, P. A. (1997). Structure–function analysis of TAF130: identification and characterization of a high-affinity TATA-binding protein interaction domain in the N terminus of yeast TAF(II)130. *Mol. Cell. Biol.* **17**, 3081–3093.
11. Banik, U., Beechem, J. M., Klebanow, E., Schroeder, S. & Weil, P. A. (2001). Fluorescence-based analyses of the effects of full-length recombinant TAF130p on the interaction of TATA box-binding protein with TATA box DNA. *J. Biol. Chem.* **276**, 49100–49109.
12. Martel, L. S., Brown, H. J. & Berk, A. J. (2002). Evidence that TAF–TATA box-binding protein interactions are required for activated transcription in mammalian cells. *Mol. Cell. Biol.* **22**, 2788–2798.
13. Kokubo, T., Swanson, M. J., Nishikawa, J. I., Hinnebusch, A. G. & Nakatani, Y. (1998). The yeast TAF145 inhibitory domain and TFIIA competitively bind to TATA-binding protein. *Mol. Cell. Biol.* **18**, 1003–1012.
14. Takahata, S., Ryu, H., Ohtsuki, K., Kasahara, K., Kawaichi, M. & Kokubo, T. (2003). Identification of a novel TATA element-binding protein binding region at the N terminus of the *Saccharomyces cerevisiae* TAF1 protein. *J. Biol. Chem.* **278**, 45888–45902.
15. Kotani, T., Miyake, T., Tsukihashi, Y., Hinnebusch, A. G., Nakatani, Y., Kawaichi, M. & Kokubo, T. (1998). Identification of highly conserved amino-terminal segments of dTAFII230 and yTAFII145 that are functionally interchangeable for inhibiting TBP–DNA interactions *in vivo* and in promoting yeast cell growth *in vivo*. *J. Biol. Chem.* **273**, 32254–32264.
16. Chitikila, C., Huisinga, K. L., Irvin, J. D., Basehoar, A. D. & Pugh, B. F. (2002). Interplay of TBP inhibitors in global transcriptional control. *Mol. Cell*, **10**, 871–882.
17. Liu, D., Ishima, R., Tong, K. I., Bagby, S., Kokubo, T. & Muhandiram, D. R. (1998). Solution structure of a TBP–TAF(II)230 complex: protein mimicry of the minor groove surface of the TATA box unwound by TBP. *Cell*, **94**, 573–583.
18. Ozer, J., Mitsouras, K., Zerby, D., Carey, M. & Lieberman, P. M. (1998). Transcription factor IIA derepresses TATA-binding protein (TBP)-associated factor inhibition of TBP–DNA binding. *J. Biol. Chem.* **273**, 14293–14300.
19. Bagby, S., Mal, T. K., Liu, D., Raddatz, E., Nakatani, Y. & Ikura, M. (2000). TFIIA-TAF regulatory interplay: NMR evidence for overlapping binding sites on TBP. *FEBS Letters*, **468**, 149–154.
20. Cheng, J. X., Floer, M., Ononaji, P., Bryant, G. & Ptashne, M. (2002). Responses of four yeast genes to changes in the transcriptional machinery are determined by their promoters. *Curr. Biol.* **12**, 1828–1832.
21. Kim, Y. J., Bjorklund, S., Li, Y., Sayre, M. H. & Kornberg, R. D. (1994). A multiprotein mediator of transcriptional activation and its interaction with the C-terminal repeat domain of RNA polymerase II. *Cell*, **77**, 599–608.
22. Johnson, K. M. & Carey, M. (2003). Assembly of a mediator/TFIID/TFIIA complex bypasses the need for an activator. *Curr. Biol.* **13**, 772–777.
23. Kim, Y., Geiger, J. H., Hahn, S. & Sigler, P. B. (1993). Crystal structure of a yeast TBP/TATA-box complex. *Nature*, **365**, 512–520.
24. Kim, J. L., Nikolov, D. B. & Burley, S. K. (1993). Co-crystal structure of TBP recognizing the minor groove of a TATA element. *Nature*, **365**, 520–527.
25. Foster, M. P., Wuttke, D. S., Clemens, K. R., Jahnke, W., Radhakrishnan, I., Tennant, L. *et al.* (1998). Chemical shift as a probe of molecular interfaces: NMR studies of DNA binding by the three amino-terminal zinc finger domains from transcription factor IIIA. *J. Biomol. NMR*, **12**, 51–71.
26. Kotani, T., Banno, K., Ikura, M., Hinnebusch, A. G., Nakatani, Y., Kawaichi, M. & Kokubo, T. (2000). A role of transcriptional activators as antirepressors for the autoinhibitory activity of TATA box binding of transcription factor IID. *Proc. Natl Acad. Sci. USA*, **97**, 7178–7183.
27. Brown, D. T. (2003). Histone H1 and the dynamic regulation of chromatin function. *Biochem. Cell. Biol.* **81**, 221–227.
28. Lian, J. B., Stein, J. L., Stein, G. S., van Wijnen, A. J., Montecino, M., Javed, A. *et al.* (2003). Runx2/Cbfa1 functions: diverse regulation of gene transcription by chromatin remodeling and co-regulatory protein interactions. *Connect. Tissue Res.* **44**, 141–148.
29. Gregory, P. D., Schmid, A., Zavari, M., Munsterkotter, M. & Horz, W. (1999). Chromatin remodelling at the PHO8 promoter requires SWI-SNF and SAGA at a step subsequent to activator binding. *EMBO J.* **18**, 6407–6414.
30. Pugh, B. F. (2000). Control of gene expression through regulation of the TATA-binding protein. *Gene*, **255**, 1–14.
31. Auble, D. T., Hansen, K. E., Mueller, C. G., Lane, W. S., Thorner, J. & Hahn, S. (1994). Mot1, a global repressor of RNA polymerase II transcription, inhibits TBP binding to DNA by an ATP-dependent mechanism. *Genes Dev.* **8**, 1920–1934.
32. Geisberg, J. V., Moqtaderi, Z., Kuras, L. & Struhl, K. (2002). Mot1 associates with transcriptionally active promoters and inhibits association of NC2 in *Saccharomyces cerevisiae*. *Mol. Cell. Biol.* **22**, 8122–8134.
33. Goppelt, A., Stelzer, G., Lottspeich, F. & Meisterernst, M. (1996). A mechanism for repression of class II gene transcription through specific binding of NC2 to TBP-promoter complexes *via* heterodimeric histone fold domains. *EMBO J.* **15**, 3105–3116.
34. Gadbois, E. L., Chao, D. M., Reese, J. C., Green, M. R. & Young, R. A. (1997). Functional antagonism between RNA polymerase II holoenzyme and global negative regulator NC2 *in vivo*. *Proc. Natl Acad. Sci. USA*, **94**, 3145–3150.
35. Kou, H., Irvin, J. D., Huisinga, K. L., Mitra, M. & Pugh, B. F. (2003). Structural and functional analysis of mutations along the crystallographic dimer interface of the yeast TATA binding protein. *Mol. Cell. Biol.* **23**, 3186–3201.

36. Nishikawa, J., Kokubo, T., Horikoshi, M., Roeder, R. G. & Nakatani, Y. (1997). *Drosophila* TAF(II)230 and the transcriptional activator VP16 bind competitively to the TATA box-binding domain of the TATA box-binding protein. *Proc. Natl Acad. Sci. USA*, **94**, 85–90.
37. Kokubo, T., Yamashita, S., Horikoshi, M., Roeder, R. G. & Nakatani, Y. (1994). Interaction between the N-terminal domain of the 230-kDa subunit and the TATA box-binding subunit of TFIID negatively regulates TATA-box binding. *Proc. Natl Acad. Sci. USA*, **91**, 3520–3524.
38. Radhakrishnan, I., Perez-Alvarado, G. C., Parker, D., Dyson, H. J., Montminy, M. R. & Wright, P. E. (1997). Solution structure of the KIX domain of CBP bound to the transactivation domain of CREB: a model for activator:coactivator interactions. *Cell*, **91**, 741–752.
39. Uesugi, M., Nyanguile, O., Lu, H., Levine, A. J. & Verdine, G. L. (1997). Induced alpha helix in the VP16 activation domain upon binding to a human TAF. *Science*, **277**, 1310–1313.
40. Kussie, P. H., Gorina, S., Marechal, V., Elenbaas, B., Moreau, J., Levine, A. J. & Pavletich, N. P. (1996). Structure of the MDM2 oncoprotein bound to the p53 tumor suppressor transactivation domain. *Science*, **274**, 948–953.
41. Mishra, A. K., Vasanthi, P. & Bhargava, P. (2003). The transcriptional activator GAL4-VP16 regulates the intra-molecular interactions of the TATA-binding protein. *J. Biosci.* **28**, 423–436.
42. Dion, V. & Coulombe, B. (2003). Interactions of a DNA-bound transcriptional activator with the TBP–TFIIA–TFIIB–promoter quaternary complex. *J. Biol. Chem.* **278**, 11495–11501.
43. Hall, D. B. & Struhl, K. (2002). The VP16 activation domain interacts with multiple transcriptional components as determined by protein–protein cross-linking *in vivo*. *J. Biol. Chem.* **277**, 46043–46050.
44. Kays, A. R. & Schepartz, A. (2002). Gal4-VP16 and Gal4-AH increase the orientational and axial specificity of TATA box recognition by TATA box binding protein. *Biochemistry*, **41**, 3147–3155.
45. Yamazaki, T., Lee, W., Revington, M., Mattiello, D. L., Dahlquist, F. W., Arrowsmith, C. H. & Kay, L. E. (1994). A suite of triple resonance NMR experiments for the backbone assignment of 15N, 13C, 2H labeled proteins with high sensitivity. *J. Am. Chem. Soc.* **116**, 11655–11666.
46. Delaglio, F., Grzesiek, S., Vuister, G. W., Zhu, G., Pfeifer, J. & Bax, A. (1995). NMRPipe: a multidimensional spectral processing system based on UNIX pipes. *J. Biomol. NMR*, **6**, 277–293.
47. Bartels, C. H., Xia, T.-H., Billeter, M., Guntert, P. & Wuthrich, K. (1995). The program XEASY for computer-supported NMR spectral analysis of biological macromolecules. *J. Biomol. NMR*, **5**, 1–10.
48. Wishart, D. S. & Sykes, B. D. (1994). The 13C chemical-shift index: a simple method for the identification of protein secondary structure using 13C chemical-shift data. *J. Biomol. NMR*, **4**, 171–180.
49. Spera, S. & Bax, A. (1991). Empirical correlation between protein backbone conformation and Ca and Cb nuclear magnetic resonance chemical shifts. *J. Am. Chem. Soc.* **113**, 5490–5492.
50. Grzesiek, S., Bax, A., Clore, G. M., Gronenborn, A. M., Hu, J. S., Kaufman, J. *et al.* (1996). The solution structure of HIV-1 Nef reveals an unexpected fold and permits delineation of the binding surface for the SH3 domain of Hck tyrosine protein kinase. *Nature Struct. Biol.* **3**, 340–345.
51. Tsukihashi, Y., Miyake, T., Kawaichi, M. & Kokubo, T. (2000). Impaired core promoter recognition caused by novel yeast TAF145 mutations can be restored by creating a canonical TATA element within the promoter region of the TUB2 gene. *Mol. Cell. Biol.* **20**, 2385–2399.
52. Stargell, L. A. & Struhl, K. (1995). The TBP–TFIIA interaction in the response to acidic activators *in vivo*. *Science*, **269**, 75–78.
53. Cadwell, R. C. & Joyce, G. F. (1992). Randomization of genes by PCR mutagenesis. *PCR Methods Appl.* **2**, 28–33.
54. Adams, A., Gottschling, D. E., Kaiser, C. A. & Stearns, T. (1997). *Methods in Yeast Genetics: A Cold Spring Harbor Laboratory Course Manual*, Cold Spring Harbor Laboratory Press, New York, NY.
55. Kraulis, P. (1991). MOLSCRIPT: a program to produce both detailed and schematic plots of protein structures. *J. Appl. Crystallog.* **24**, 946–950.

Edited by P. Wright

(Received 19 February 2004; received in revised form 2 April 2004; accepted 7 April 2004)

Supplementary Material comprising one Figure is available on Science Direct